

 Open access • Posted Content • DOI:10.1101/2021.09.03.21262852

## The international and intercontinental spread and expansion of antimicrobial-resistant *Salmonella* Typhi — [Source link](#)

Kesia Esther da Silva, Arif Mohammad Tanmoy, Agila Kumari Pragasam, Junaid Iqbal ...+25 more authors

**Institutions:** [Stanford University](#), [Erasmus University Medical Center](#), [Aga Khan University](#), [University of Glasgow](#) ...+7 more institutions

**Published on:** 07 Sep 2021 - [medRxiv](#) (Cold Spring Harbor Laboratory Press)

**Topics:** [Salmonella typhi](#)

Related papers:

- [A genomic snapshot of Salmonella enterica serovar Typhi in Colombia.](#)
- [Phylogenetic Analysis Indicates a Longer Term Presence of the Globally Distributed H58 Haplotype of Salmonella Typhi in Southern India.](#)
- [Phylogenomics and antimicrobial resistance of salmonella typhi and paratyphi a, b and c in england, 2016–2019](#)
- [Salmonella enterica Serovar Typhi in Bangladesh: Exploration of Genomic Diversity and Antimicrobial Resistance.](#)
- [Emergence of ceftriaxone resistant Salmonella enterica serovar Typhi in Eastern India.](#)

Share this paper:    

View more about this paper here: <https://typeset.io/papers/the-international-and-intercontinental-spread-and-expansion-d3uh452oym>

1 **The international and intercontinental spread and expansion of antimicrobial-resistant**

2 ***Salmonella* Typhi**

3

4 Kesia Esther da Silva<sup>1,\*</sup>, Arif Mohammad Tanmoy<sup>2,3,\*</sup>, Agila Kumari Pragasam<sup>4,\*</sup>, Junaid Iqbal<sup>5,\*</sup>,  
5 Mohammad Saiful Islam Sajib<sup>2,6</sup>, Ankur Mutreja<sup>7</sup>, Balaji Veeraraghavan<sup>4</sup>, Dipesh Tamrakar<sup>8</sup>,  
6 Farah Naz Qamar<sup>5</sup>, Gordon Dougan<sup>9,10</sup>, Isaac Bogoch<sup>11</sup>, Jessica C Seidman<sup>12</sup>, Jivan Shakya<sup>13,14</sup>,  
7 Krista Vaidya<sup>13</sup>, Megan E. Carey<sup>10</sup>, Rajeev Shrestha<sup>15</sup>, Seema Irfan<sup>16</sup>, Stephen Baker<sup>9,10</sup>, Steve P.  
8 Luby<sup>1</sup>, Yanjia Cao<sup>1</sup>, Zoe Anne Dyson<sup>10,17,18,19</sup>, Denise O. Garrett<sup>12</sup>, Jacob John<sup>20</sup>, Gagandeep  
9 Kang<sup>21</sup>, Yogesh Hooda<sup>2,22</sup>, Samir K. Saha<sup>2,23</sup>,<sup>†</sup> Senjuti Saha<sup>2</sup>,<sup>†</sup> Jason R. Andrews<sup>1†</sup>

10

11 <sup>1</sup>Division of Infectious Diseases and Geographic Medicine, Stanford University, Stanford, CA,  
12 USA.

13 <sup>2</sup>Child Health Research Foundation, Dhaka, Bangladesh.

14 <sup>3</sup>Department of Medical Microbiology and Infectious Diseases, Erasmus University Medical  
15 Center, Rotterdam, The Netherlands.

16 <sup>4</sup>Department of Clinical Microbiology, Christian Medical College, Vellore, India.

17 <sup>5</sup>Department of Pediatrics and Child Health, Aga Khan University, Karachi, Pakistan.

18 <sup>6</sup>Institute of Biodiversity, Animal Health and Comparative Medicine, University of Glasgow,  
19 Glasgow, UK.

20 <sup>7</sup>Cambridge Institute of Therapeutic Immunology & Infectious Disease (CITIID) Department of  
21 Medicine, University of Cambridge, Cambridge, UK.

22 <sup>8</sup>Department of Community Medicine, Kathmandu University School of Medical Sciences, Nepal.

23 <sup>9</sup>University of Cambridge School of Clinical Medicine, Cambridge Biomedical Campus,  
24 Cambridge, UK.

25 <sup>10</sup>Department of Medicine, University of Cambridge School of Clinical Medicine, Cambridge  
26 Biomedical Campus, Cambridge, UK.

27 <sup>11</sup>Department of Medicine, University of Toronto, Toronto, Canada.

28 <sup>12</sup>Applied Epidemiology, Sabin Vaccine Institute, Washington, DC, USA.

29 <sup>13</sup>Dhulikhel Hospital, Kathmandu University Hospital, Kavrepalanchok, Nepal.

30 <sup>14</sup>Central Department of Microbiology at Tribhuvan University, Kirtipur, Nepal.

31 <sup>15</sup>Department of Pharmacology, Kathmandu University School of Medical Sciences, Dhulikhel,  
32 Nepal.

33 <sup>16</sup>Department of Pathology and Microbiology, Aga Khan University Hospital, Karachi, Pakistan.

34 <sup>17</sup>London School of Hygiene & Tropical Medicine, London, UK.

35 <sup>18</sup>Department of Infectious Diseases, Central Clinical School, Monash University, Melbourne,  
36 Victoria, Australia.

37 <sup>19</sup>Wellcome Sanger Institute, Wellcome Genome Campus, Hinxton, Cambridge, UK.

38 <sup>20</sup>Department of Community Health, Christian Medical College, Vellore, India.

39 <sup>21</sup>The Wellcome Trust Research Laboratory, Division of Gastrointestinal Sciences, Christian  
40 Medical College, Vellore, India.

41 <sup>22</sup>MRC Laboratory Molecular Biology, Cambridge, UK.

42 <sup>23</sup>Department of Microbiology, Dhaka Shishu Hospital, Dhaka, Bangladesh.

43 \* Contributed Equally

44 † Contributed Equally

45

46 **Word Count (intro, results, discussion): 2,913**

47 **Abstract Word Count: 109**

48 **Figures: 5**

49 **Tables: 0**

50

51 **Correspondence:**

52 Jason R. Andrews

53 Division of Infectious Diseases and Geographic Medicine

54 Stanford University School of Medicine

55 Biomedical Innovations Building, Room 3458

56 Stanford, CA 94025, USA

57 Email: [jandr@stanford.edu](mailto:jandr@stanford.edu)

58 Phone: +1 650 497 2679

59

60 **Abstract**

61

62 The emergence of increasingly antimicrobial-resistant (AMR) *Salmonella enterica* serovar Typhi  
63 (*S. Typhi*) threatens to undermine effective treatment and control. Here, aiming to investigate the  
64 temporal and geographic patterns of emergence and spread of AMR *S. Typhi*, we sequenced  
65 3,489 *S. Typhi* isolated from prospective surveillance in South Asia and combined these with a  
66 global collection of 4,169 *S. Typhi* genomes. Our analysis revealed that independent acquisition  
67 of plasmids and homoplastic mutations conferring AMR have occurred repeatedly in multiple  
68 lineages of *S. Typhi*, predominantly arising in South Asia. We found evidence of frequent  
69 international and intercontinental transfers of AMR *S. Typhi*, followed by rapid expansion and  
70 replacement of antimicrobial-susceptible clades.

71

72

73 **Introduction**

74 Typhoid fever, the disease caused by *Salmonella enterica* serovar Typhi (*S. Typhi*), remains a  
75 major worldwide public health concern (1). The organism causes 11 million illnesses and  
76 >100,000 deaths annually (2,3). The highest typhoid fever incidence rates occur in South Asia,  
77 which contains 70% of the global disease burden, but substantial morbidity and mortality also  
78 occur in sub-Saharan Africa, Southeast Asia, and Oceania. In the pre-antimicrobial era, the case  
79 fatality rate of typhoid fever was around 15%, but morbidity and mortality declined dramatically  
80 following the introduction of chloramphenicol in the 1940s, followed by ampicillin and  
81 trimethoprim-sulfamethoxazole in the 1960s (4,5).

82  
83 The effectiveness of antimicrobial therapy for typhoid fever has been repeatedly threatened by  
84 the emergence and expansion of organisms that exhibit resistance to the principal antimicrobials.  
85 Multi-drug resistant (MDR) variants, harboring genes encoding resistance to ampicillin,  
86 chloramphenicol, and trimethoprim-sulfamethoxazole first emerged in the 1970s; subsequently,  
87 a single lineage (H58; 4.3.1) was introduced into sub-Saharan Africa and Southeast Asia from  
88 South Asia and became globally dominant (6,7). The genes facilitating resistance to these  
89 specific antimicrobials were originally only located on IncHI1 plasmids but later also became  
90 integrated into the chromosome. The fluoroquinolones were initially highly effective against  
91 early MDR *S. Typhi* organisms and became the mainstay of therapy in South Asia in the 1990s.  
92 However, fluoroquinolone non-susceptible isolates started to emerge in the mid 1990s and,  
93 within 20 years, the majority of *S. Typhi* in South Asia contained mutations in the quinolone  
94 resistance-determining regions (QRDR) (4) (8). In 2016, a large outbreak of *S. Typhi* containing  
95 plasmid-mediated resistance to third generation cephalosporins and fluoroquinolones and

96 chromosomally located genes encoding the MDR phenotype was identified in Pakistan and  
97 termed extensively drug-resistant (XDR) (9). More recently, a single polymorphism in the AcrB  
98 efflux pump conferring resistance to azithromycin was found to have independently arisen in  
99 multiple lineages of *S. Typhi*, threatening the efficacy of all oral antibiotic antimicrobials for  
100 typhoid treatment (10). Taken together, *S. Typhi* has exhibited resistance to all oral drugs known  
101 to be effective for its treatment, although it has not yet been identified in the same clone.

102  
103 Typhoid conjugate vaccines (TCV) have recently proven effective for disease prevention, and the  
104 World Health Organization recommends prioritized introduction in countries with a high burden  
105 of antimicrobial resistant *S. Typhi* (11). However, given the current trajectory of antimicrobial  
106 resistant (AMR) in *S. Typhi* waiting until a high AMR burden is present within a country to  
107 introduce typhoid vaccines may ill-advised. Understanding the historical emergence, expansion  
108 and geographic spread of antimicrobial resistant *S. Typhi* may yield insights into where resistant  
109 strains might spread and how quickly they will become dominant within populations.

110  
111 Here, we leveraged prospective, population-based typhoid surveillance studies from four of the  
112 highest burden countries in South Asia: Bangladesh, India, Nepal and Pakistan. We sequenced  
113 3,489 *S. Typhi* organisms isolated over a six-year period, and these data were combined with a  
114 global collection of >4,000 additional genomes sequences to investigate the emergence and  
115 geographical spread of AMR *S. Typhi* over the past three decades.

116

## 117 **Results**

118 *Genotypic diversity and phylogenetic structure of S. Typhi in South Asia*

119 A total of 3,489 *S. Typhi* isolates from four countries (Bangladesh, India, Nepal, and Pakistan)  
120 collected between 2014 and 2019 were sequenced. Genotype analysis identified 29 distinct  
121 genotypes (**Figure S1**). The majority of isolates (2,474; 70.9%) belonged to genotype 4.3.1  
122 (haplotype H58). The major sublineages of H58 (lineage I and lineage II) were common, with  
123 H58 lineage I (genotype 4.3.1.1) dominant in Bangladesh and Pakistan, and H58 lineage II  
124 (genotype 4.3.1.2) the most common genotype in India and Nepal. Among non-H58 isolates, the  
125 most common subclades were subclade 3.2.2 (190; 5.5%), 3.3.2 (161; 4.6%), 2.3.3 (140; 4.0%),  
126 2.5 (123; 3.5%), and 3.3.1 (85; 2.4%).

127  
128 We identified multiple, phylogenetically linked sub-lineages shared across South Asia (**Figure**  
129 **S2**), most regularly between Bangladesh, Nepal, and India. Within the H58 isolates, *S. Typhi*  
130 4.3.1.2 isolates formed distinct clades with intermingled isolates from India and Nepal, while  
131 4.3.1.3 isolates, identified predominantly in Bangladesh, clustered with few isolates from India. In  
132 contrast, the H58 isolates from Pakistan largely clustered independently and was dominated by a  
133 monophyletic XDR clade (4.3.1.1.P1).

134

### 135 *Global phylogenetic structure and determinants of antimicrobial resistance*

136 To provide additional context for the 3,489 *S. Typhi* new South Asian genome sequences, and  
137 better understand temporal and spatial distribution of lineages and antimicrobial resistance, we  
138 constructed a further phylogeny incorporating an additional 4,169 *S. Typhi* sequences from  
139 organisms isolated from 1905 to 2018 from >70 countries (**Figure 1**). Overall, the new  
140 sequences clustered with previously sequenced South Asian isolates, generating distinct  
141 geographic structure. Genotype 4.3.1 formed a large subclade. Primary clades 2, 3 and 4 were



142 distributed across continents with limited isolates outside these clades. Notably, four subclades  
143 (2.3.3, 2.5, 3.2.2, and 3.3) were dominant in South Asia, accounting for 75.7% of all non-H58  
144 organisms.

145  
146 We classified isolates as multidrug-resistant if they containing genes conferring resistance to  
147 ampicillin (*bla*<sub>TEM-1</sub>), chloramphenicol (*catA1*), and trimethoprim-sulfamethoxazole (*dfrA7*, *sul1*,  
148 or *sul2*). From 2000 onwards, we observed a declining trend in MDR isolates in Bangladesh and  
149 India, a stable low proportion (<5%) in Nepal, and an increasing proportion in Pakistan and  
150 Africa (**Figure S3a**). Acquired resistance genes that contribute to the MDR phenotype were  
151 identified in 26.8% of the isolates of the global genome collection, including 98.4% of the H58  
152 isolates, in comparison to just 1.6% of the non-H58 isolates (1.1.1, 2.5.1, 3.1.1, 3.2.1, 3.4, 4).  
153 Among these rare non-H58 multidrug-resistant isolates, resistance was almost exclusively  
154 entirely plasmid-mediated (96.9%). In contrast, for H58 isolates we observed that plasmid-  
155 mediated resistance was persistent in the H58 isolates in the 1990s, but from 2000 onward was  
156 less frequent, with most MDR isolates containing chromosomal insertions of drug-resistance  
157 genes (75.2%).

158  
159 In contrast to the temporal trends in MDR, there was a consistent rise in the proportion of global  
160 *S. Typhi* that were fluoroquinolone non-susceptible (FQNS), primarily associated with mutations  
161 *gyrA*, *gyrB*, *parC*, and *parE* (**Figure S3b**). The most dramatic increase in FQNS *S. Typhi*  
162 occurred in Bangladesh, exceeding 85% by early 2000, followed by India, Pakistan, and Nepal,  
163 reaching >95% in all four South Asian countries. FQNS *S. Typhi* increased from <20% in 2007  
164 year to >60% by 2011 in Southeast Asia. In Africa, this increase occurred more recently,

165 originating in 2010. Overall, we found that QRDR mutations were significantly more common in  
166 the H58 isolates (89.1%) compared with other lineages (45.4%) ( $p < 0.0001$ ). From 2010  
167 onwards, an increasing number of isolates containing multiple QRDR mutations; >10% of all  
168 isolates harbored three mutations (**Figure S3**). Among the novel genome sequences, 437 were  
169 ‘triple mutants’ (Table S3), which are highly associated with full resistance and failure to  
170 respond to fluoroquinolone therapy (12). The majority (402/437; 92%) of these organisms  
171 occurred in H58 lineage II (4.3.1.2) in India and Nepal; the second most common (15/437; 3.4%)  
172 triple mutant genotype was 3.3 and predominantly isolated in India.

173  
174 Susceptibility to fluoroquinolones can be further reduced via plasmid-mediated acquisition of  
175 *qnr* genes. We identified *qnrS* in two non-H58 isolates (genotype 3) and 686 H58 isolates that  
176 included genotype 4.3.1 (n = 3), 4.3.1.1 (n = 5), 4.3.1.P1 (n = 550), and 4.3.1.3 (n = 125). Most  
177 H58 lineage I isolates from Pakistan were XDR (4.3.1.P1) carrying the previously identified  
178 composite transposon containing *bla*<sub>TEM-1</sub>, *catA1*, *dfrA7*, *sul1*, *sul2* inserted in the chromosome,  
179 and *bla*<sub>CTX-M-15</sub> and *qnrS* associated with an IncY plasmid (9). Azithromycin resistance, conferred  
180 by *acrB* mutations (R717Q and R717L), was identified in 54 isolates across eight different  
181 genotypes including genotype 4.3.1 (n = 1), 4.3.1.1 (n = 31), 4.3.1.2 (n = 5), 4.3.1.3 (n = 2), and  
182 non-H58 isolates comprising, genotype 2.3.3 (n = 2), 3.2.2 (n = 9), 3.3.2 (n = 3) and 3.5.4 (n =  
183 1).

184  
185 *Antimicrobial resistance and growth of the effective population size*

186 To investigate how the AMR has shaped the effective population size of *S. Typhi*, we generated  
187 timed phylogenies and modeled the effective population size of antimicrobial susceptible and

188 antimicrobial resistant organisms over time. To minimize the effect of location and lineage, we  
189 focused on the largest haplotype (H58) and performed analyses within countries, evaluating key  
190 AMR determinants. In Nepal, we found that the effective population size ( $N_e$ ) of *S. Typhi*  
191 containing one or two QRDR mutations rose steadily from 2000, beginning to decline from  
192 2017, while triple mutants have steadily increased from 2010 (**Figure 2**). In Pakistan, the  $N_e$  of  
193 non-XDR H58 *S. Typhi* increased from 2000 until around 2015 and began to fall; XDR  
194 organisms emerged and have been rapidly growing in frequency since 2016, eclipsing the  
195 effective population of non-XDR organisms by 2018. In Bangladesh, the  $N_e$  of H58 had slowly  
196 declined from around 2010; however, azithromycin-resistant organisms emerged in 2013 with a  
197 corresponding increase in  $N_e$ . In all three settings, organisms with key AMR conferring  
198 mutations or genes appear to be replacing their susceptible (or, in the case of fluoroquinolones,  
199 less-resistant) counterparts.

200

### 201 *The global phylogeography of S. Typhi*

202 Using country of sampling as a discrete trait, we generated dated phylogenies to reconstruct the  
203 evolutionary history and geographic spread of H58 lineage and the four 4 common non-H58  
204 genotypes. These five genotypes accounted for 75% of all isolates from the past decade. The  
205 mean nucleotide substitution rates for each lineage are described in **Table S4**.

206

207 Phylogeographic reconstruction of H58 isolates (4.3.1, 4.3.1.1, 4.3.1.1.P1, 4.3.2.1 and 4.3.1.3)  
208 estimated that the time of most recent common ancestor (tMRCA) of all contemporary H58 *S.*  
209 *Typhi* strains existed around 37 years ago (1984). The distribution of isolates and the tree  
210 topology are consistent with at least 138 international transfer events, including multiple

211 introductions within South Asia and dissemination from South Asia into Southeast Asia and  
212 Africa, as well as many travel-related cases identified in the U.K. and U.S. (**Figure 3, Figure 4**).  
213 The distribution of QRDR mutations within the phylogeny demonstrated that these resistance-  
214 conferring mutations have arisen independently on at least 80 distinct occasions. We also  
215 predicted that ciprofloxacin-resistant triple mutant isolates most likely originated in India around  
216 1996 and were introduced into Pakistan between 2005 and 2013 and into Nepal on at least three  
217 occasions (2003-2015). Furthermore, we identified frequent transmissions of international  
218 transfer of MDR isolates (n = 33), with multiple introductions from South Asia followed by local  
219 expansion. In addition, the phylogeographic analyses also showed that the Pakistani XDR  
220 lineage (genotype 4.3.1.1.P1) emerged around 2015 and has been subsequently identified on  
221 multiple occasions in United Kingdom and United States.

222  
223 The major non-H58 clades also acquired AMR loci and spread within and from South Asia.  
224 Genotype 2.3.3 circulated predominantly in Bangladesh but spread to Pakistan and India within  
225 the past 30 years (**Figure S5**). QRDR mutations within genotype 2.3.3 have emerged  
226 independently on at least three occasions. Genotype 2.5, which may have circulated in India for  
227 >100 years (**Figure S6**), has been transferred to sub-Saharan Africa and Nepal multiple times,  
228 including two instances with strains containing QRDR mutations since 2015. Genotype 3.2.2  
229 organisms originating from Bangladesh were observed in South Asia only. We observed a single  
230 instance of transfer from Bangladesh to Nepal and ongoing local expansion. In contrast, we  
231 found that these organisms have been regularly transferred from Bangladesh to India (**Figure**  
232 **S7**). Transfer events included at least four recent introductions of FQNS organisms between  
233 2006 and 2017. The most recent common ancestor of genotype 3.3 was estimated to have been

234 from India >200 years ago (**Figure S8**), but moved extensively across South Asia, establishing  
235 large subclades in Bangladesh and Nepal, before progressing to sub-Saharan Africa, the Middle  
236 East, and Southeast Asia. Genotype 3.3 organisms with QRDR mutations have moved from India  
237 to Nepal on multiple occasions.

238

239 Overall, our analysis identified evidence for 197 introduction events between countries, of which  
240 138 were intracontinental and 59 were intercontinental (**Figure 5**). The most common  
241 international transmission events were within South Asia and from South Asia to Southeast Asia,  
242 East and Southern Africa. We estimated that resistance-conferring mutations to fluoroquinolones  
243 or azithromycin have independently emerged on at least 101 separate occasions within the last 30  
244 years, mostly in South Asian countries (n = 94), and occasionally arising in Southeast Asia,  
245 Africa and South America. In addition, isolates carrying QRDR mutations were recently  
246 transferred between countries on at least 119 independent occasions.

247

## 248 **Discussion**

249 This analysis of *S. Typhi* genome sequences reveals that the acquisition through plasmid  
250 acquisition or frequent, homoplastic mutations occurring across multiple lineages, has been  
251 accompanied by expansion and international spread of AMR *S. Typhi* clones. We identified  
252 numerous international and intercontinental transfers of *S. Typhi* over the past thirty years, with  
253 the majority associated with AMR phenotypes. Once introduced to a new setting, AMR *S. Typhi*  
254 become quickly fixed, as broadly exemplified with fluoroquinolone non-susceptible clades in  
255 multiple countries and XDR *S. Typhi* in Pakistan. This rapid emergence, spread and fixation of  
256 AMR in *S. Typhi* suggests that making decisions regarding TCV introduction via current AMR

257 data may miss a critical window for prevention. Specifically, we found that South Asia continues  
258 to be an important hub for AMR generation in *S. Typhi* and that the clones emerging here  
259 regularly move internationally, underscoring the need for resources to support typhoid control in  
260 this region.

261  
262 Our data are consistent with recent studies suggesting that MDR *S. Typhi*—strains resistant to  
263 the classical first line drugs— is now generally on the decline in South Asia (13,14). The decline  
264 of MDR *S. Typhi* in Asia has been accompanied by a decrease in the proportion of isolates  
265 carrying IncHI1 plasmids (except for Pakistan, where the MDR decline abruptly reversed amid  
266 the emergence of the XDR lineage). In our study, MDR was principally associated with H58  
267 carrying chromosomally integrated AMR genes. The integration of AMR genes into the *S. Typhi*  
268 chromosome remains a concern, as it provides a mechanism for stable vertical transmission of  
269 MDR phenotypes (6,15). In contrast to South Asia, MDR typhoid associated with H58 and non-  
270 H58 isolates appears to be increasing in parts of Africa, with outbreaks being reported in the last  
271 decade (16,17).

272  
273 QRDR mutations have independently arisen in all *S. Typhi* lineages due to sustained  
274 fluoroquinolone exposure. Nearly all of organisms containing QRDR mutations appear to have  
275 arisen in South Asia, and many have spread regionally and globally. Notably, our analysis  
276 revealed that highly fluoroquinolone resistant *S. Typhi* triple mutants have recently emerged in  
277 six different genotypes, including H58 lineage (4.3.1), lineage I (4.3.1.1), lineage II (4.3.1.2),  
278 and non-H58 isolates (3.3). Our phylogeography analysis suggests that these isolates most likely  
279 originated in India and disseminated to neighboring countries including Nepal and Pakistan.

280

281 The recent emergence and spread of resistance to third-generation cephalosporins and  
282 azithromycin further complicates typhoid fever treatment (8,9). Within three years of its first  
283 recognition, the XDR genotype (4.3.1.1.P1) became the dominant genotype circulating in  
284 Pakistan. The same sub-clade has been isolated from travelers returning from Pakistan to  
285 Canada, United Kingdom and United States (18,19). Recently, there have been reports of non-  
286 travel associated cases of 4.3.1.1.P1 XDR *S. Typhi* in the United States, suggestive of local  
287 transmission following importation (19). The XDR genotype has been typically associated with a  
288 composite MDR transposon inserted in the chromosome and by the acquisition of an IncY  
289 plasmid carrying *bla*<sub>CTX-M-15</sub> and *qnrS1* (9). However, a recent study reported multiple  
290 integrations of *bla*<sub>CTX-M-15</sub> from the IncY plasmid into the chromosome of XDR *S. Typhi* isolates  
291 (20). Chromosomal integration of *bla*<sub>CTX-M-15</sub> may lessen its impact fitness cost, making it more  
292 likely that resistance will be maintained even in the absence of selection pressure in a  
293 comparable manner to the MDR gene cassette integration (15,20).

294

295 At present, all XDR *S. Typhi* strains identified have been susceptible to azithromycin and  
296 carbapenems (19). Concerningly, azithromycin-resistant *S. Typhi* have recently been reported in  
297 Bangladesh, India, Pakistan, Nepal and Singapore (10,21,22), arising from mutations in *acrB*.  
298 These mutations have arisen independently multiple times in distinct lineages (10). To date,  
299 XDR *S. Typhi* isolates containing mutations in *acrB* have not yet been identified. Such  
300 organisms would preclude effective treatment with established oral antimicrobials, which could  
301 lead to increased hospitalization rates, greater morbidity and mortality.

302

303 Our findings should be interpreted within the context of the limitations of the available data.  
304 While this analysis included the largest collection of novel *S. Typhi* genome sequences to date,  
305 there remains underrepresentation of sequences from several regions, including  
306 disproportionately small numbers from many countries in sub-Saharan Africa and Oceania where  
307 typhoid is endemic. Even in countries with more dense sampling, most isolates were derived  
308 from a small number of surveillance sites and may not be representative of the distribution of  
309 circulating strains. Because *S. Typhi* genomes only cover a fraction of all typhoid fever cases,  
310 phylogenies are highly incomplete; our estimates for AMR-conferring homoplastic mutations  
311 and international transfers represent lower bounds like may substantially underestimate their true  
312 frequency. These circumstances highlight the need for expanding genomic surveillance for  
313 enteric pathogens to provide a more comprehensive window into the emergence, expansion and  
314 spread of antimicrobial-resistant organisms.

315  
316 The present study highlights the sustained emergence and geographic spread of AMR *S. Typhi*  
317 strains, with evidence of frequent international exportation. This observation underscores the  
318 importance of approaching typhoid fever control and antimicrobial resistance as a global rather  
319 than local problem. The recent emergence of XDR and azithromycin-resistant *S. Typhi* creates  
320 greater urgency for rapidly expanding prevention measures, including use of TCV and  
321 improvements to water and sanitation infrastructure, in typhoid-endemic countries. Such  
322 measures are needed in countries where AMR prevalence among *S. Typhi* isolates is currently  
323 high, but given the propensity for international spread, should not be restricted to such setting.

324

325 **Methods**



326 *Bacterial isolates*

327 This study included *S. Typhi* isolates obtained from the Surveillance for Enteric Fever in Asia  
328 Project (SEAP; Bangladesh, Nepal, and Pakistan; 2016-2019), Etiologies of Acute Febrile Illness  
329 Study (Nepal; 2014-2016), and Surveillance for Enteric Fever in India Project (SEFI; 2017-2019).  
330 The study methodologies have been previously described (23–25). In brief, participants for these  
331 studies included individuals of all ages presenting to study site facilities with febrile illness.  
332 These included 5 facilities in Dhaka, Bangladesh, 18 facilities across 16 cities in India, 11  
333 facilities across 3 cities in Nepal and two hospitals and a university laboratory network in  
334 Karachi, Pakistan. Across these studies, there were a total of 9,945 blood culture-confirmed  
335 typhoid cases. From these, we selected a country-stratified sample of 3,489 *S. Typhi* isolates for  
336 sequencing. Details on the sampling for each country are available in the Appendix.

337

338 *Whole-genome sequencing*

339 Whole-genome sequencing (WGS) was performed at the Wellcome Trust Sanger Institute using  
340 the Illumina HiSeq2500 platform (Illumina, San Diego, CA, USA) to generate paired-end reads  
341 of 100–150 bp in length, and at a commercial service in Bangalore and at the Wellcome Trust  
342 Research Laboratory in the Christian Medical College using the Illumina MiSeq platform  
343 (Illumina, San Diego, CA, USA). Sequence data quality was checked using FastQC v0.11.9 to  
344 remove low quality reads (26). We summarized all quality indicators using MultiQC v1.7 (27).  
345 Species identification was confirmed with Kraken2 (28), and the *Salmonella in silico* Typing  
346 Resource (SISTR) was used for WGS-based serotyping (29). Short Read Sequence Typing for  
347 Bacterial Pathogens (SRST2) (30) was used to map known alleles and identify MLSTs directly

348 from reads according to the *Salmonella enterica* MLST scheme

349 (<https://pubmlst.org/salmonella/>).

350

351 *Mapping and SNP analysis*

352 Paired-end Illumina reads were mapped to the *S. Typhi* CT18 (accession no. AL513382)

353 reference chromosome sequence using RedDog mapping pipeline v1beta.11 ([https://github.com/](https://github.com/katholt/reddog)

354 [katholt/reddog](https://github.com/katholt/reddog)). RedDog uses Bowtie2 v2.4.1 (31) to map reads to the reference genome, and

355 SAMtools v1.10 (32) to identify SNPs that have a phred quality score above 30, and to filter out

356 those SNPs supported by less than five reads, or with 2.5x the average read depth that represent

357 putative repeated sequences, or those that have ambiguous base calls. For each SNP that passes

358 these criteria in any one isolate, consensus base calls for the SNP locus were extracted from all

359 genomes mapped, with those having phred quality scores under 20 being treated as unknown

360 alleles and represented with a gap character.

361

362 Chromosomal SNPs with confident homozygous calls (phred score above 20) in >95% of the

363 genomes mapped (representing a ‘soft’ core genome) were concatenated to form an alignment of

364 alleles using the RedDog python script parseSNPtable.py with parameters -m cons, aln and -c

365 0.95 and SNPs called in prophage regions and repetitive sequences (354 kb; ~7.4% of bases) in

366 the CT18 reference chromosome, as defined previously (33) were excluded to form an alignment

367 of 14,901 variant sites. SNPs occurring in recombinant regions were detected by Gubbins v2.4.1

368 (34) and excluded resulting in a final alignment of 11,978 chromosomal SNPs. The SNP data

369 were used to assign all isolates to previously defined genotypes according to an extended *S.*

370 *Typhi* genotyping framework using the GenoTyphi python script

371 (<https://github.com/katholt/genotyphi>) (33). To provide global context, additional *S. Typhi*  
372 genomes (9,12,17,33,35–41) were subjected to both SNP calling, recombination filtering, and  
373 genotyping as described above, resulting in an alignment of 28,897 chromosomal SNPs.

374

#### 375 *Phylogenetic analyses*

376 Maximum likelihood (ML) phylogenetic trees were inferred from the chromosomal SNP  
377 alignments using RAxML v8.2.10 (42) (command `raxmlHPC-PTHREADS`). A generalized time-  
378 reversible model and a Gamma distribution was used to model site-specific rate variation (GTR+  
379  $\Gamma$  substitution model; GTRGAMMA in RAxML) with 100 bootstrap pseudoreplicates used to  
380 assess branch support for the ML phylogeny. We selected the single tree with the highest  
381 likelihood score as the best tree. The resulting phylogenies were visualized and annotated using  
382 the iTOL v5 online version (43).

383

#### 384 *Temporal and phylogeographic analysis*

385 To investigate dates of emergence and geographical transfers, we inferred timed phylogenies  
386 using globally and temporally representative samples. First, we used TempEst v1.5 to assess  
387 temporal structure by conducting a regression of the root-to-tip branch distances of the tree as a  
388 function of the sampling time (44), which was confirmed by a clustered permutation test using  
389 *BactDating* (45). For the non-H58 isolates, we estimated the best-fit models, tree topology,  
390 evolutionary rates, and phylogeography by using a Bayesian Markov chain Monte Carlo  
391 (MCMC) method with the software package BEAST2 v2.6.2 (46). Separate trees were fit for  
392 each of the most common non-H58 lineages (2.3.3, 2.5, 3.2.2, and 3.3). Isolates from each

393 lineage were selected based on temporal, geographic and phylogenetic diversity, as described in  
394 detail in the Appendix.

395

396 For the BEAST analysis, a GTR+ $\Gamma$  substitution model was selected, and the sampling times (tip  
397 dates) were defined as the year of isolation to calibrate the molecular clock. We tested support  
398 for a strict clock for each lineage using the relaxed clock test in *treedater*, and the strict clock  
399 was rejected in each instance (47). We therefore constructed time-phylogenies using coalescent  
400 exponential population priors with a relaxed clock (uncorrelated lognormal distribution) (6,17).

401 Three independent runs were performed to ensure convergence, and were combined with  
402 LogCombiner, following removal of the first 10 million steps from each as burn-in. The effective  
403 sample sizes (ESSs) of the parameters were estimated to be >200 for all independent runs of the  
404 analysis. The trees were summarized in a maximum clade credibility (MCC) target tree using the  
405 Tree Annotator program v2.4.7. The time of the most recent common ancestor (tMRCA)  
406 estimates were calculated as the years before the most recent sampling dates. Phylogeographical  
407 reconstruction was obtained by the continuous-time Markov Chain process over discrete  
408 sampling locations implemented in BEAST. The final trees were visualized using FigTree v1.4  
409 (<http://tree.bio.ed.ac.uk/software>). For H58, we had 4,761 isolates, which precluded temporal and  
410 phylogeographic analysis using BEAST due to computational constraints. To avoid significant  
411 down-sampling of isolates, we used the *treedater* R package (47) with an uncorrelated, relaxed  
412 molecular clock to estimate the timed phylogeny for H58, which yielded a tMRCA matching a  
413 root-to-tip based analysis using *BactDating* and consistent with previously published estimates  
414 (6). We included all H58 sequences available in our collection to improve accuracy of the timed  
415 phylogeny and phylogeographic analysis. We reconstructed the ancestral state of nodes using the

416 maximum parsimony approach with the *Phangorn* R package, considering important events with  
417 a location probability of >0.5 between connected nodes. For visualization purposes, we selected  
418 a smaller subset of sequences to depict in a dated phylogenetic tree. For all phylogeographic  
419 analyses, we considered a geographic transfer when the most probable location between two  
420 connected nodes (or between a node and a tip) differed, and we considered the time window of  
421 transfer as the date range between the nodes (or between the node and tip). The geospatial  
422 transmissions of lineage strains from the phylogeographic reconstructions were analyzed and  
423 visualized using ArcMap 10.7.1 (<https://desktop.arcgis.com/en/arcmap/>).

424

#### 425 *Non-parametric phylodynamic inference of effective population size*

426 To evaluate the historical effective population size for H58 lineage strains, we used the time-  
427 stamped H58 tree to estimate the effective population size through time using  
428 the *skygrowth* package (<https://github.com/mrc-ide/skygrowth>). We pruned the timed  
429 phylogenies by country and antimicrobial resistance pattern to compare the effective population  
430 sizes of antimicrobial resistant and sensitive populations.

431

#### 432 *AMR associated genes detection and plasmid replicon analysis*

433 ARIBA (Antimicrobial Resistance Identifier by Assembly) v2.10.0 and CARD database v1.1.8  
434 (<https://card.mcmaster.ca/home>) were used to investigate antimicrobial resistance gene content.  
435 Point mutations in the quinolone resistance determining region (QRDR) of the DNA-gyrase  
436 *gyrA/B* and topoisomerase-IV *parC/E* genes, associated with reduced susceptibility to  
437 fluoroquinolones and quinolone resistance genes (*qnrS*) were also detected using ARIBA.  
438 Isolates were defined as being MDR if resistance genes were detected by ARIBA in the beta-

439 lactam, trimethoprim/sulphonamide and chloramphenicol classes. Plasmid replicons were  
440 identified using ARIBA and the PlasmidFinder database (30).

441

#### 442 *Data availability*

443 Illumina sequence data was submitted to the European Nucleotide Archive. Sequence data from  
444 4,169 *S. Typhi* strains from previous studies were also included for global context raw sequence  
445 data for these isolates are available in European Nucleotide Archive. Details and individual  
446 accession numbers of sequence data included in our analysis have been included in Tables S1  
447 and S2.

448

#### 449 *Ethics statement*

450 Ethical approval for the parent studies were obtained from the Bangladesh Institute of Child  
451 Health Ethical Review Committee, Christian Medical College Institutional Review Board, Nepal  
452 Health Research Council, Aga Khan University Hospital Ethics Committee and Pakistan  
453 National Ethics Committee, Stanford University Institutional Review Board, and U.S. Centers  
454 for Disease Control and Prevention. Informed written consent and clinical information were  
455 taken from adult participants and legal guardians of child participants.

456

#### 457 *Acknowledgements*

458 This work was supported by a grant from the Bill and Melinda Gates Foundation (grant number  
459 INV-008335).

460

461

## 462   **References**

- 463   1.     Dougan G, Baker S. *Salmonella enterica* Serovar Typhi and the Pathogenesis of Typhoid  
464     Fever . *Annu Rev Microbiol.* 2014;
- 465   2.     Antillón M, Warren JL, Crawford FW, Weinberger DM, Kürüm E, Pak GD, et al. The  
466     burden of typhoid fever in low- and middle-income countries: A meta-regression  
467     approach. *PLoS Negl Trop Dis.* 2017;
- 468   3.     Stanaway JD, Reiner RC, Blacker BF, Goldberg EM, Khalil IA, Troeger CE, et al. The  
469     global burden of typhoid and paratyphoid fevers: a systematic analysis for the Global  
470     Burden of Disease Study 2017. *Lancet Infect Dis.* 2019;19(4):369–81.
- 471   4.     Andrews JR, Qamar FN, Charles RC, Ryan ET. Extensively Drug-Resistant Typhoid —  
472     Are Conjugate Vaccines Arriving Just in Time? *N Engl J Med* [Internet]. 2018 Oct  
473     12;379(16):1493–5. Available from: <https://doi.org/10.1056/NEJMp1803926>
- 474   5.     Mogasale V, Maskery B, Ochiai RL, Lee JS, Mogasale V V., Ramani E, et al. Burden of  
475     typhoid fever in low-income and middle-income countries: A systematic, literature-based  
476     update with risk-factor adjustment. *Lancet Glob Heal.* 2014;
- 477   6.     Wong VK, Baker S, Pickard DJ, Parkhill J, Page AJ, Feasey NA, et al. Phylogeographical  
478     analysis of the dominant multidrug-resistant H58 clade of *Salmonella* Typhi identifies  
479     inter-and intracontinental transmission events. *Nat Genet.* 2015;
- 480   7.     Dyson ZA, Klemm EJ, Palmer S, Dougan G. Antibiotic resistance and typhoid. *Clin Infect*  
481     *Dis.* 2019;
- 482   8.     Hooda Y, Sajib MSI, Rahman H, Luby SP, Bondy-Denomy J, Santosham M, et al.  
483     Molecular mechanism of azithromycin resistance among typhoidal *Salmonella* strains in  
484     Bangladesh identified through passive pediatric surveillance. *PLoS Negl Trop Dis.* 2019;
- 485   9.     Klemm EJ, Shakoor S, Page AJ, Qamar FN, Judge K, Saeed DK, et al. Emergence of an  
486     extensively drug-resistant *Salmonella enterica* serovar typhi clone harboring a  
487     promiscuous plasmid encoding resistance to fluoroquinolones and third-generation  
488     cephalosporins. *MBio.* 2018;
- 489   10.    Sajib MSI, Tanmoy AM, Hooda Y, Rahman H, Andrews JR, Garrett DO, et al. Tracking  
490     the emergence of azithromycin resistance in multiple genotypes of typhoidal salmonella.  
491     *MBio.* 2021;12(1):1–12.
- 492   11.    World Health Organization. Typhoid vaccines: WHO position paper, March 2018 –

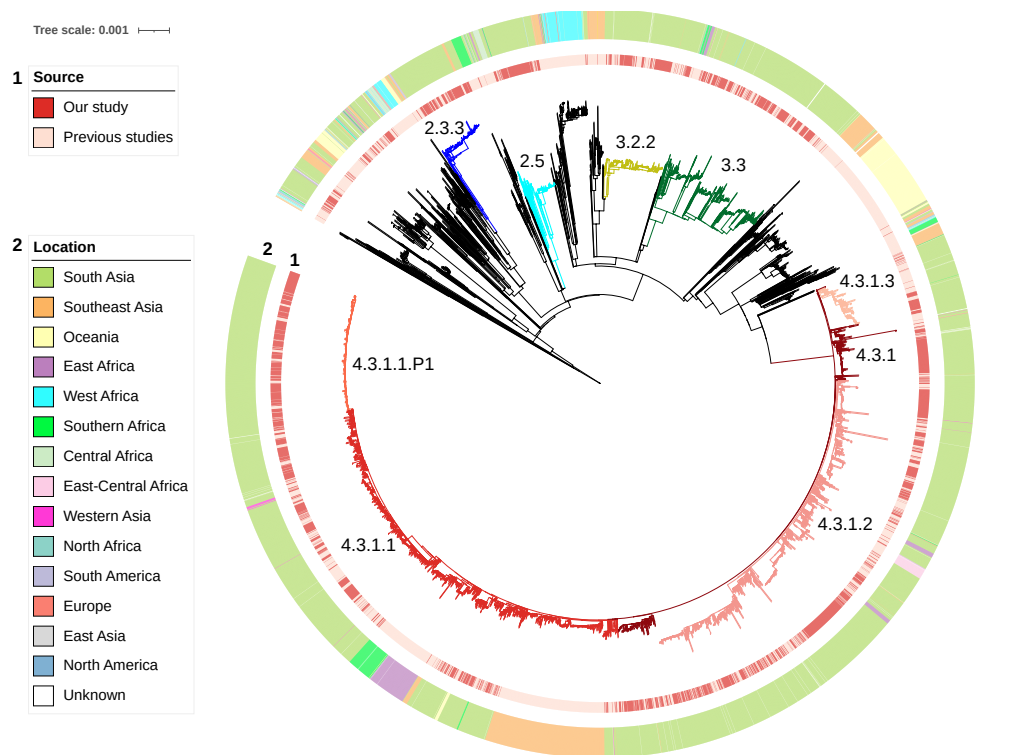
- 493 Recommendations. *Vaccine* [Internet]. 2019;37(2):214–6. Available from:  
494 <https://www.sciencedirect.com/science/article/pii/S0264410X18304912>
- 495 12. Thanh DP, Karkey A, Dongol S, Thi NH, Thompson CN, Rabaa MA, et al. A novel  
496 ciprofloxacin-resistant subclade of h58. *Salmonella typhi* is associated with  
497 fluoroquinolone treatment failure. *Elife*. 2016;
- 498 13. Carter AS, Luby SP, Garrett DO. Introducing Typhoid Conjugate Vaccine in South Asia:  
499 Lessons From the Surveillance for Enteric Fever in Asia Project. *Clin Infect Dis*  
500 [Internet]. 2020 Dec 1;71(Suppl 3):S191–5. Available from:  
501 <https://pubmed.ncbi.nlm.nih.gov/33258930>
- 502 14. Balaji V, Kapil A, Shastri J, Pragasam AK, Gole G, Choudhari S, et al. Longitudinal  
503 Typhoid Fever Trends in India from 2000 to 2015. *Am J Trop Med Hyg* [Internet].  
504 2018/07/24. 2018 Sep;99(3\_Suppl):34–40. Available from:  
505 <https://pubmed.ncbi.nlm.nih.gov/30047367>
- 506 15. Holt KE, Baker S, Weill FX, Holmes EC, Kitchen A, Yu J, et al. *Shigella sonnei* genome  
507 sequencing and phylogenetic analysis indicate recent global dissemination from Europe.  
508 *Nat Genet*. 2012;44(9):1056–9.
- 509 16. Consortium IT, Wong VK, Holt KE, Okoro C, Baker S, Pickard DJ, et al. Molecular  
510 Surveillance Identifies Multiple Transmissions of Typhoid in West Africa. *PLoS Negl*  
511 *Trop Dis* [Internet]. 2016 Sep 22;10(9):e0004781–e0004781. Available from:  
512 <https://pubmed.ncbi.nlm.nih.gov/27657909>
- 513 17. Park SE, Pham DT, Boinett C, Wong VK, Pak GD, Panzner U, et al. The phylogeography  
514 and incidence of multi-drug resistant typhoid fever in sub-Saharan Africa. *Nat Commun*.  
515 2018;
- 516 18. Eshaghi A, Zittermann S, Bharat A, Mulvey MR, Allen VG, Patel SN. Importation of  
517 Extensively Drug-Resistant *Salmonella enterica* Serovar Typhi  
518 Cases in Ontario, Canada. *Antimicrob Agents Chemother* [Internet]. 2020 Apr  
519 21;64(5):e02581-19. Available from: <http://aac.asm.org/content/64/5/e02581-19.abstract>
- 520 19. Health Alert Network C. Extensively Drug-Resistant *Salmonella Typhi* Infections Among  
521 U.S. Residents Without International Travel. *HAN Arch*. 2021;(CDCHAN-00439):0–5.
- 522 20. Nair S, Chattaway M, Langridge GC, Gentle A, Day M, Ainsworth E V, et al. ESBL-



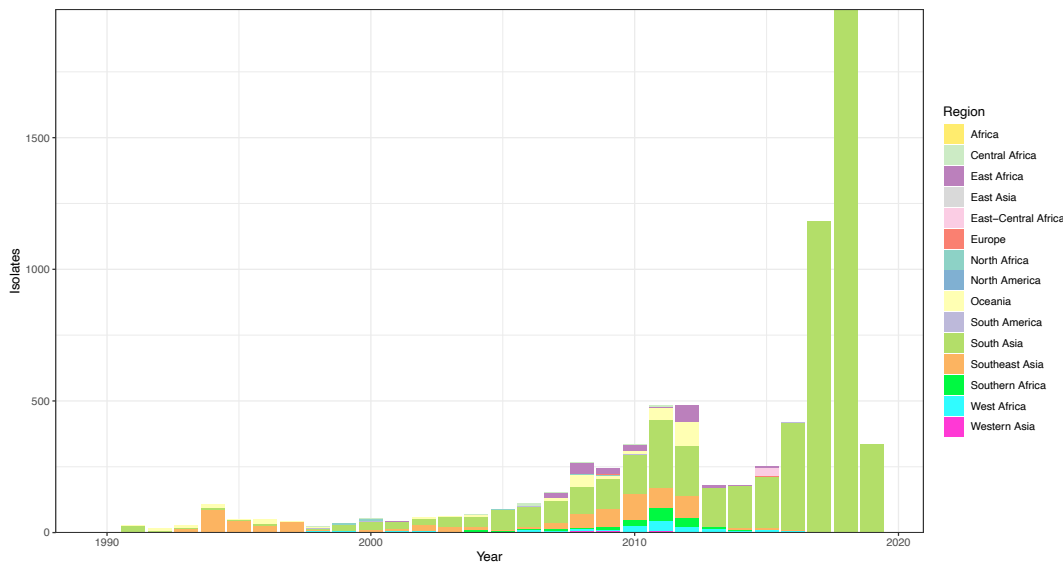
- 524 producing strains isolated from imported cases of enteric fever in England and Wales  
525 reveal multiple chromosomal integrations of bla CTX-M-15 in XDR Salmonella Typhi . J  
526 Antimicrob Chemother. 2021;1–8.
- 527 21. Octavia S, Chew KL, Lin RT, Teo JW. Azithromycin-Resistant *Salmonella*  
528 *enterica* Serovar Typhi AcrB-R717Q/L, Singapore. *Emerg Infect Dis J* [Internet].  
529 2021;27(2):624. Available from: [https://wwwnc.cdc.gov/eid/article/27/2/20-3874\\_article](https://wwwnc.cdc.gov/eid/article/27/2/20-3874_article)
- 530 22. Carey ME, Jain R, Yousuf M, Maes M, Dyson ZA, Thu TNH, et al. Spontaneous  
531 Emergence of Azithromycin Resistance in Independent Lineages of *Salmonella* Typhi in  
532 Northern India. *Clin Infect Dis*. 2021;72(5):e120–7.
- 533 23. Andrews JR, Vaidya K, Bern C, Tamrakar Di, Wen S, Madhup S, et al. High Rates of  
534 Enteric Fever Diagnosis and Lower Burden of Culture-Confirmed Disease in Peri-urban  
535 and Rural Nepal. *J Infect Dis*. 2018;
- 536 24. Andrews JR, Barkume C, Yu AT, Saha SK, Qamar FN, Garrett D, et al. Integrating  
537 Facility-Based Surveillance with Healthcare Utilization Surveys to Estimate Enteric Fever  
538 Incidence: Methods and Challenges. *J Infect Dis*. 2018;218(Suppl 4):S268–76.
- 539 25. Barkume C, Date K, Saha SK, Qamar FN, Sur Di, Andrews JR, et al. Phase i of the  
540 Surveillance for Enteric Fever in Asia Project (SEAP): An Overview and Lessons  
541 Learned. *J Infect Dis*. 2018;218(Suppl 4):S188–94.
- 542 26. Andrews S. Babraham Bioinformatics - FastQC A Quality Control tool for High  
543 Throughput Sequence Data. *Soil*. 1973.
- 544 27. Ewels P, Magnusson M, Lundin S, Källner M. MultiQC: Summarize analysis results for  
545 multiple tools and samples in a single report. *Bioinformatics*. 2016;
- 546 28. Wood DE, Lu J, Langmead B. Improved metagenomic analysis with Kraken 2. *Genome*  
547 *Biol*. 2019;
- 548 29. Yoshida CE, Kruczkiewicz P, Laing CR, Lingohr EJ, Gannon VPI, Nash JHE, et al. The  
549 salmonella in silico typing resource (SISTR): An open web-accessible tool for rapidly  
550 typing and subtyping draft salmonella genome assemblies. *PLoS One*. 2016;
- 551 30. Inouye M, Dashnow H, Raven LA, Schultz MB, Pope BJ, Tomita T, et al. SRST2: Rapid  
552 genomic surveillance for public health and hospital microbiology labs. *Genome Med*.  
553 2014;
- 554 31. Langmead B, Salzberg S. Bowtie2. *Nat Methods*. 2013;

- 555 32. Li H, Handsaker B, Wysoker A, Fennell T, Ruan J, Homer N, et al. The Sequence  
556 Alignment/Map format and SAMtools. *Bioinformatics*. 2009;
- 557 33. Wong VK, Baker S, Connor TR, Pickard D, Page AJ, Dave J, et al. An extended  
558 genotyping framework for *Salmonella enterica* serovar Typhi, the cause of human  
559 typhoid. *Nat Commun*. 2016;
- 560 34. Croucher NJ, Page AJ, Connor TR, Delaney AJ, Keane JA, Bentley SD, et al. Rapid  
561 phylogenetic analysis of large samples of recombinant bacterial whole genome sequences  
562 using Gubbins. *Nucleic Acids Res*. 2015;
- 563 35. Ingle DJ, Nair S, Hartman H, Ashton PM, Dyson ZA, Day M, et al. Informal genomic  
564 surveillance of regional distribution of *Salmonella* Typhi genotypes and antimicrobial  
565 resistance via returning travellers. *PLoS Negl Trop Dis*. 2019;
- 566 36. Rahman SIA, Dyson ZA, Klemm EJ, Khanam F, Holt KE, Chowdhury EK, et al.  
567 Population structure and antimicrobial resistance patterns of salmonella typhi isolates in  
568 Urban Dhaka, Bangladesh from 2004 to 2016. *PLoS Negl Trop Dis*. 2020;
- 569 37. Tanmoy AM, Westeel E, De Bruyne K, Goris J, Rajoharison A, Sajib MSI, et al.  
570 *Salmonella enterica* serovar typhi in Bangladesh: Exploration of genomic diversity and  
571 antimicrobial resistance. *MBio*. 2018;
- 572 38. Britto CD, Dyson ZA, Mathias S, Bosco A, Dougan G, Jose S, et al. Persistent circulation  
573 of a fluoroquinolone-resistant *Salmonella enterica* Typhi clone in the Indian subcontinent.  
574 *J Antimicrob Chemother*. 2020;
- 575 39. Pragasam AK, Pickard D, Wong V, Dougan G, Kang G, Thompson A, et al. Phylogenetic  
576 Analysis Indicates a Longer Term Presence of the Globally Distributed H58 Haplotype of  
577 *Salmonella* Typhi in Southern India. *Clin Infect Dis*. 2020;
- 578 40. Britto CD, Dyson ZA, Duchene S, Carter MJ, Gurung M, Kelly DF, et al. Laboratory and  
579 molecular surveillance of paediatric typhoidal *Salmonella* in Nepal: Antimicrobial  
580 resistance and implications for vaccine policy. *PLoS Negl Trop Dis*. 2018;
- 581 41. Dyson ZA, Thanh DP, Bodhidatta L, Mason CJ, Srijan A, Rabaa MA, et al. Whole  
582 Genome Sequence Analysis of *Salmonella* Typhi Isolated in Thailand before and after the  
583 Introduction of a National Immunization Program. *PLoS Negl Trop Dis*. 2017;
- 584 42. Stamatakis A. RAXML version 8: A tool for phylogenetic analysis and post-analysis of  
585 large phylogenies. *Bioinformatics*. 2014;

- 586 43. Letunic I, Bork P. Interactive Tree Of Life (iTOL) v4: recent updates and new  
587 developments. *Nucleic Acids Res.* 2019;
- 588 44. Rambaut A, Lam TT, Carvalho LM, Pybus OG. Exploring the temporal structure of  
589 heterochronous sequences using TempEst (formerly Path-O-Gen). *Virus Evol.* 2016;
- 590 45. Didelot X, Croucher NJ, Bentley SD, Harris SR, Wilson DJ. Bayesian inference of  
591 ancestral dates on bacterial phylogenetic trees. *Nucleic Acids Res [Internet].* 2018 Dec  
592 14;46(22):e134–e134. Available from: <https://pubmed.ncbi.nlm.nih.gov/30184106>
- 593 46. Drummond AJ, Rambaut A. BEAST: Bayesian evolutionary analysis by sampling trees.  
594 *BMC Evol Biol.* 2007;
- 595 47. Volz EM, Frost SDW. Scalable relaxed clock phylogenetic dating. *Virus Evol [Internet].*  
596 2017 Jul 1;3(2). Available from: <https://doi.org/10.1093/ve/vex025>  
597  
598  
599  
600  
601  
602  
603  
604  
605  
606  
607  
608  
609  
610  
611



612



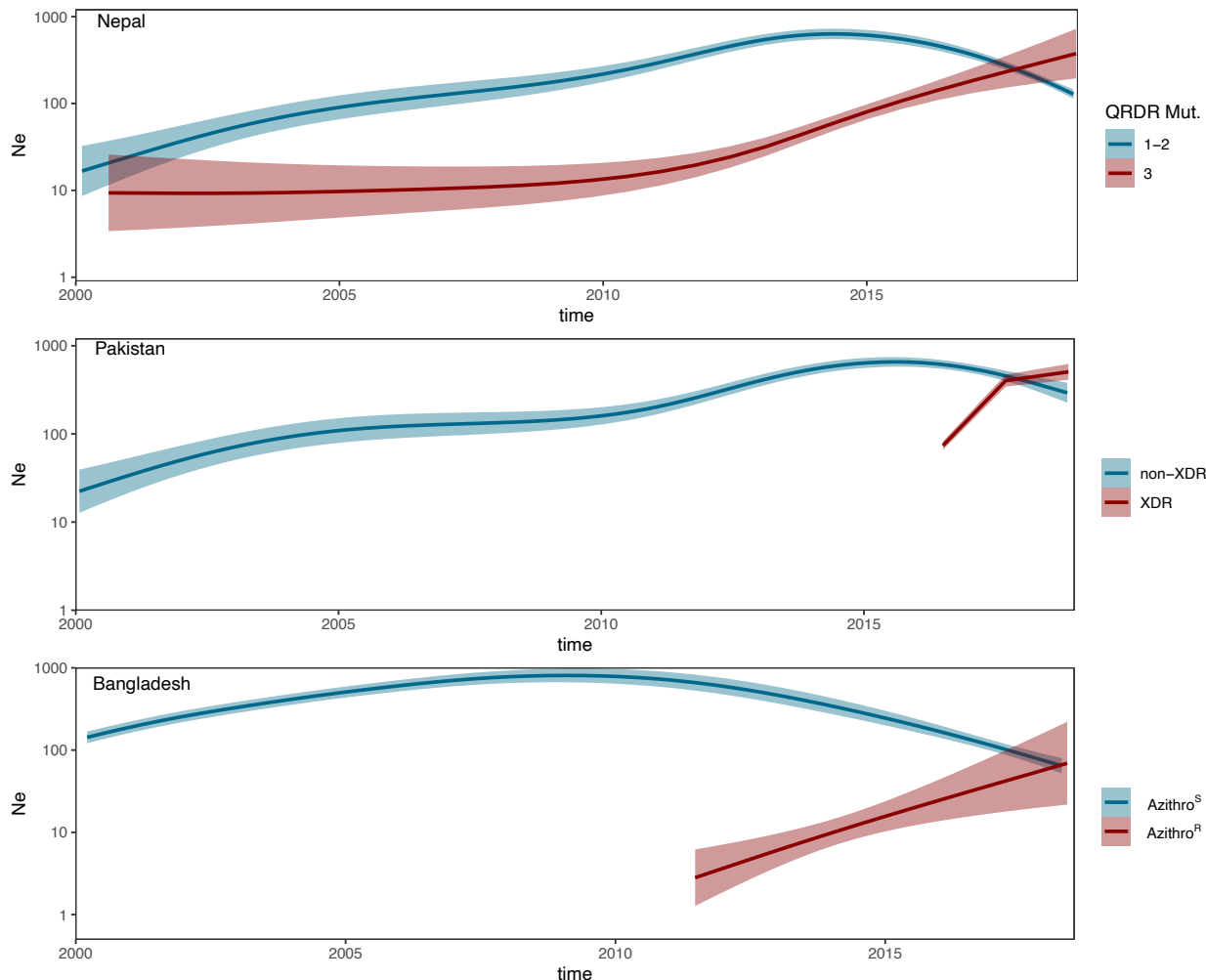
613

614 **Figure 1.** Global phylogeny of *Salmonella Typhi*. **(a)** Maximum likelihood tree of 7,658 *S. Typhi*  
615 isolates from the global collection. Branch colors indicate the lineages 2.3.3 (blue), 2.5 (turquoise),  
616 3.2.2 (yellow), 3.3 (green), 4.3.1 (dark red), 4.3.1.1 (red), 4.3.1.1.P1 (orange), 4.3.1.2 (pink),  
617 4.3.1.3 (salmon) and other non-H58 (black). The inner ring indicates the source. The outer ring  
618 indicates the region of isolation. The scale bar indicates nucleotide substitutions per site **(b)**  
619 Temporal distribution of sequenced *S. Typhi* isolates by region.

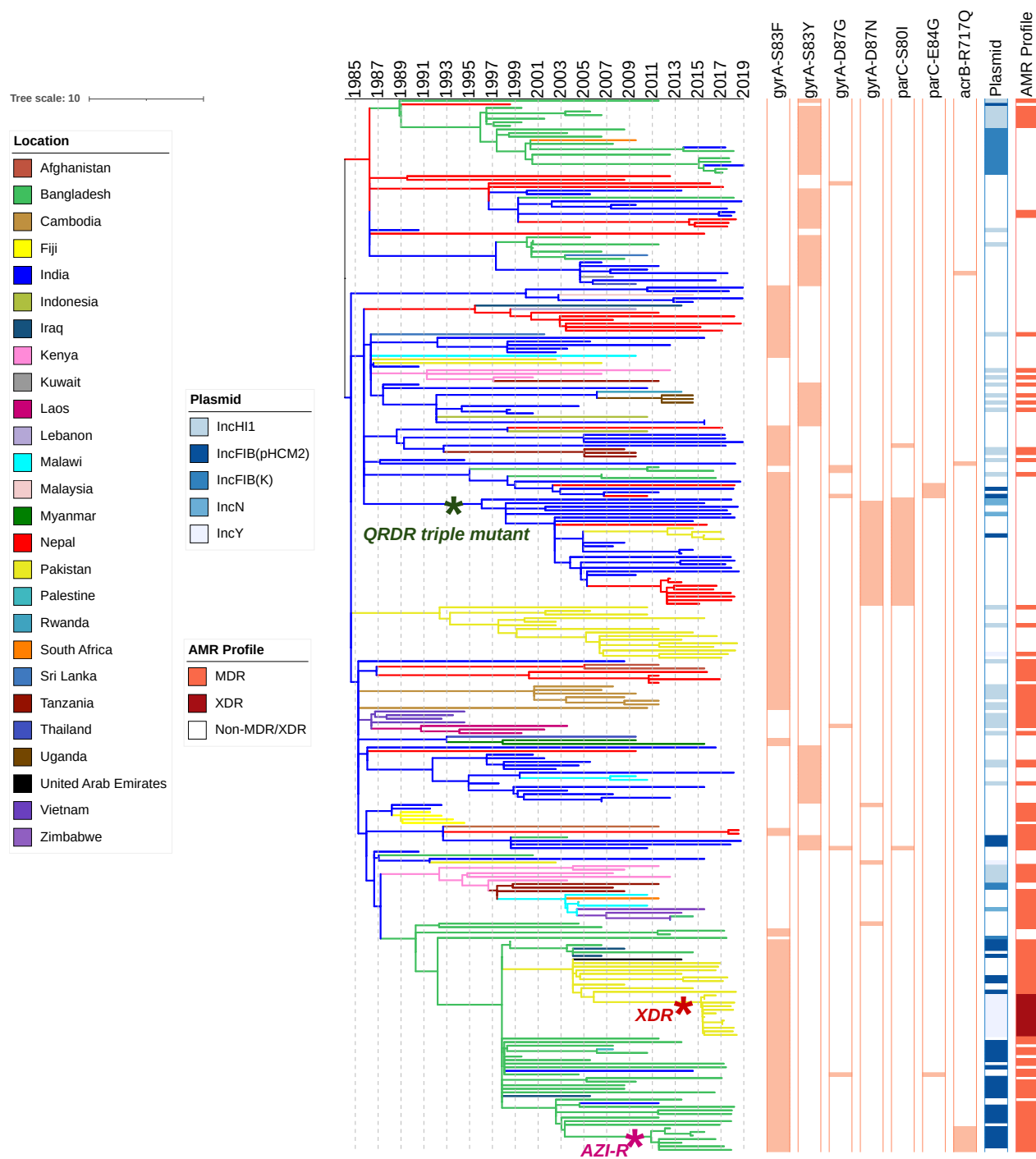
620

621

622



623  
624 **Figure 2.** The effective population size ( $N_e$ ) of H58 lineages according to antimicrobial resistance  
625 genotype in Nepal, Pakistan and Bangladesh. In Nepal, strains containing 1-2 mutations in the  
626 quinolone resistance determining region (QRDR) were compared with those containing 3  
627 mutations. In Pakistan, extensively drug-resistant (XDR) strains were compared with non-XDR  
628 strains. In Bangladesh, strains containing *acrB* mutations conferring azithromycin-resistance were  
629 compared with those not containing the mutations. Light shading represents the 95% high  
630 probability density (HPD) intervals of the estimates.  
631

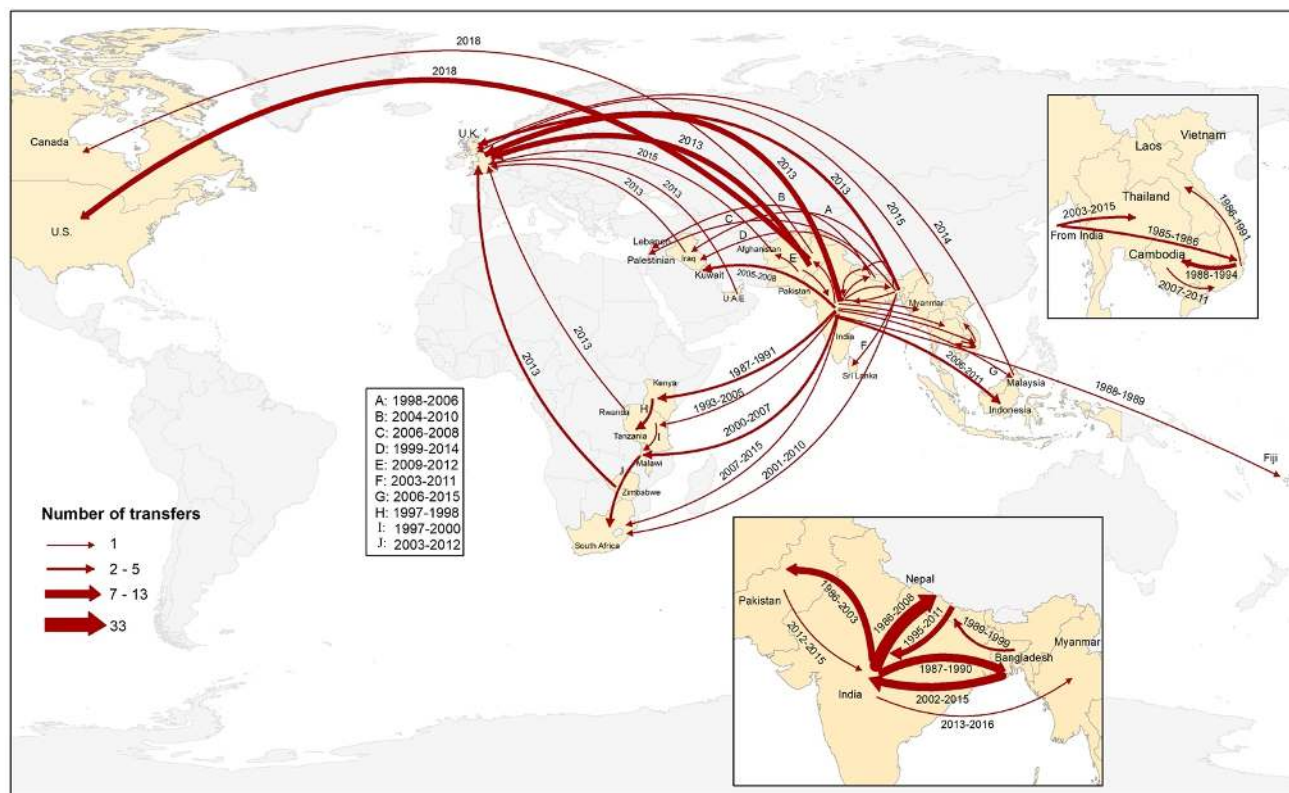


632

633

634 **Figure 3.** Phylogeography and global expansion of genotype 4.3.1 (H58) *S. Typhi* isolates. Timed  
 635 phylogenetic tree of genotype 4.3.1 *S. Typhi* isolates. The branch lengths are scaled in years and  
 636 are colored according to the location of the most probable ancestor of descendant nodes. The scale  
 637 bar indicates nucleotide substitutions per site.

638



639  
640

641 **Figure 4.** Geographical transfers within lineage 4.3.1 (H58) inferred from ancestral state  
642 reconstruction of the timed phylogenetic tree. The size of each arrow is scaled to the estimated  
643 number of transfers between the countries. Dates indicate the estimated first transfer between each  
644 pair of countries.

645

646

647

648

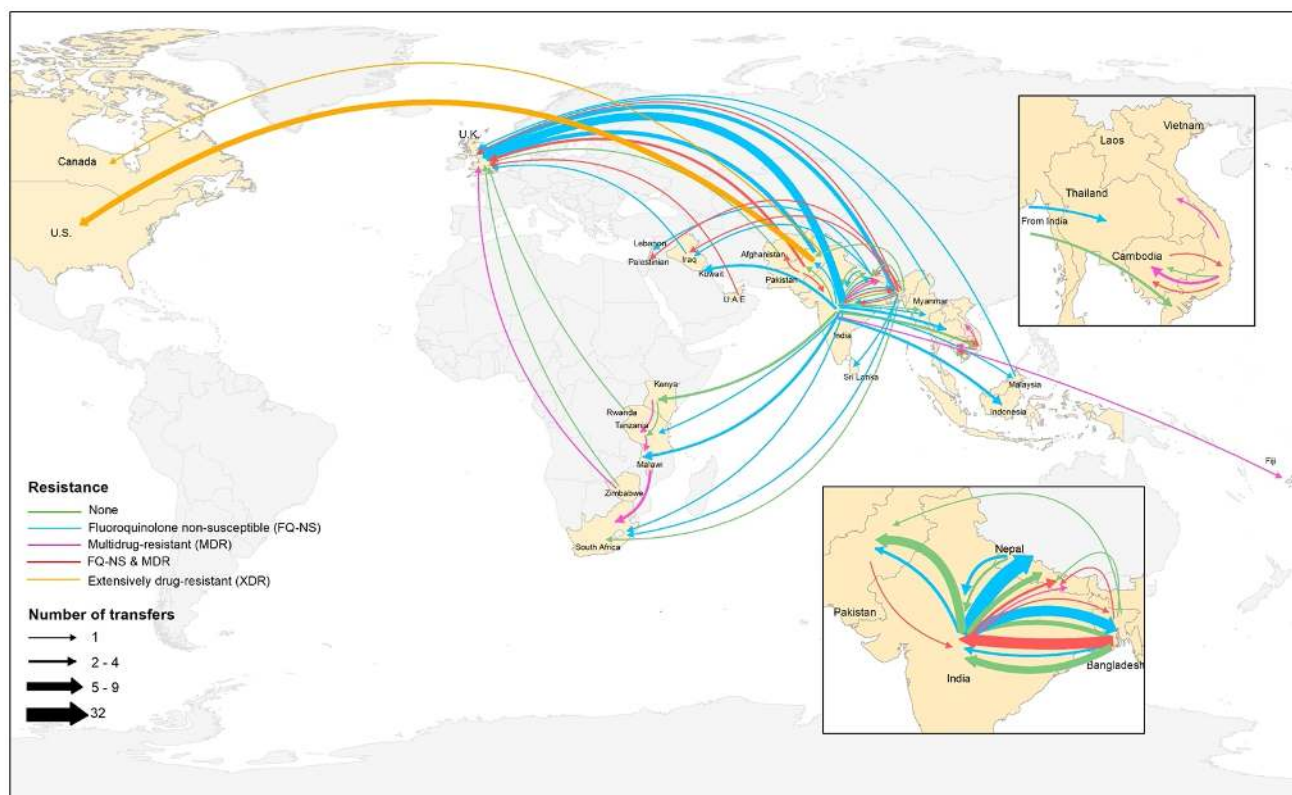
649

650

651

652





653

654

655 **Figure 5.** Major geographical transfers from 1990 onwards within the non-H58 and H58 lineages,  
656 inferred from the phylogenetic trees. The size of each arrow indicates the relative number of likely  
657 transfers between the countries. Arrow colors indicate antimicrobial resistance pattern.

658

659

660

661

662

663

664

665

666